7-18-2003

Chemical characterization of ambient aerosol collected during the northeast monsoon season over the Arabian Sea: Labile-Fe(II) and other trace metals

Anne M. Johansen
Central Washington University

Michael R. Hoffmann
California Institute of Technology

Recommended Citation

Johansen, A. M. (2003). Chemical characterization of ambient aerosol collected during the northeast monsoon season over the Arabian Sea: Labile-Fe(II) and other trace metals. Journal of Geophysical Research, 108(D14). https://doi.org/10.1029/2002jd003280

Chemical characterization of ambient aerosol collected during the northeast monsoon season over the Arabian Sea: Labile-Fe(II) and other trace metals

Anne M. Johansen
Department of Chemistry, Central Washington University, Ellensburg, Washington, USA

Michael R. Hoffmann
Environmental Science and Engineering, California Institute of Technology, Pasadena, California, USA

Received 3 December 2002; revised 26 February 2003; accepted 24 March 2003; published 18 July 2003.

[1] Ambient aerosol samples were collected over the Arabian Sea during the month of March of 1997, aboard the German R/V *Sonne*, as part of the German Joint Global Ocean Flux Study (JGOFS) project. This is the third study in a series of analogous measurements taken over the Arabian Sea during different seasons of the monsoon. Dichotomous high-volume collector samples were analyzed for ferrous iron immediately after collection, while trace metals, anions, and cations were determined upon return to the laboratory. The main crustal component was geochemically well represented by the average crustal composition and amounted to 5.94 ± 3.08 $\mu g\ m^{-3}$. An additional crustal constituent of clay-like character, rich in water-soluble Ca and Mg, was seen in the fine fraction in air masses of Arabian origin. Total ferrous iron concentrations varied from 3.9 to 17.2 ng m^{-3} and averaged 9.8 ± 3.4 ng m^{-3}, with 87.2% of Fe(II) present in the fine aerosol fraction. Fe(II) concentrations accounted for on average 1.3 ± 0.5% of the total Fe. While ferrous iron in the coarse fraction appeared to be correlated with the main crustal component, the fine Fe(II) fraction exhibited a more complex behavior. The anthropogenic contribution to the aerosol, as traced by Pb, Zn, and some anions and cations, was found to be considerably larger, especially during the first 10 days of this cruise, than in previously collected samples from the inter-monsoon and southwest monsoon of 1995. *INDEX TERMS:* 0305 Atmospheric Composition and Structure: Aerosols and particles (0345, 4801); 0365 Atmospheric Composition and Structure: Troposphere—composition and chemistry; 4801 Oceanography: Biological and Chemical: Aerosols (0305); 4805 Oceanography: Biological and Chemical: Biogeochemical cycles (1615); 4875 Oceanography: Biological and Chemical: Trace elements; *KEYWORDS:* ferrous iron, trace metals, aerosol particles, Indian Ocean

Citation: Johansen, A. M., and M. R. Hoffmann, Chemical characterization of ambient aerosol collected during the northeast monsoon season over the Arabian Sea: Labile-Fe(II) and other trace metals, *J. Geophys. Res.*, *108*(D14), 4408, doi:10.1029/2002JD003280, 2003.

1. Introduction

[2] The present study is part of a larger set of field observations collected over the Arabian Sea to determine the chemical composition of atmospheric aerosol particles during different seasons of the monsoon [*Johansen et al.*, 1999; *Siefert et al.*, 1999].

[3] The northern Indian Ocean is subject to a strong biannual reversal pattern in the low-level winds associated with the Indian monsoon [*Ackerman and Cox*, 1989; *Findlater*, 1969, 1971; *Middleton*, 1986a, 1986b]. The monsoon flow pattern, which is largely driven by the heat gradient between the Indian subcontinent and the ocean, is typified by southwest winds during the Northern Hemisphere summer and northeast winds during the Northern Hemisphere winter. The inter-monsoon is classified as the period between the northeast and the southwest monsoons when no predominant wind pattern exists. Two previous studies of the southwest monsoon and inter-monsoon showed that the direction of the airflow over the Arabian Sea affects both the abundance and composition of the aerosols [*Johansen et al.*, 1999; *Siefert et al.*, 1999]. These studies found that during the southwest monsoon the air is mainly marine derived, originating from the southwestern Indian Ocean, while during the inter-monsoon the air masses contain a consider-able amount of crustal and anthropogenic material originating mainly from the Arabian Peninsula and other parts of the Middle East. The present study used measurements of trace metals to study the hypothesis that anthropogenic influences on aerosol composition will be enhanced during the northeast monsoon, when air masses originating from the Indian subcon-

0148-0227/03/2002JD003280

tinent are advected over the Arabian Sea. Furthermore, the aerosol matrix's effect on iron speciation will be investigated in comparison to our findings from the southwest monsoon and inter-monsoon.

[4] A number of investigators [*Ansmann et al.*, 2000; *Jayaraman et al.*, 1998; *Lelieveld et al.*, 2001; *Moorthy et al.*, 1999, 2001, 1998, 1997; *Rao et al.*, 2001; *Rao and Devara*, 2001; *Satheesh and Krishna Moorthy*, 1997; *Satheesh et al.*, 1998; *Venkataraman et al.*, 2002, 2001] have studied the optical characteristics and size distributions of aerosols over the Indian Ocean during the northeast monsoon in several Indian Ocean Experiments (INDOEX) between 1996 and 1999. The above studies found that the average aerosol optical depth for the visible wavelength region was as high as 0.5 near the western coast of India, and in the range of 0.2–0.4 over the Arabian Sea, and 0.1 and less over the Indian Ocean. For comparison, the aerosol optical depth reported for the Atlantic Ocean ranged from 0.04 to 0.25 [*Hoppel et al.*, 1990].

[5] Previous measurements of trace chemical species from the Indian Ocean have confirmed the large spatial and seasonal variabilities. *Savoie et al.* [1987] sampled nitrate, NSS-sulfate and mineral aerosol during the northeast monsoon and spring inter-monsoon of 1979 and found a strong gradient in the concentrations of the measured species, decreasing toward the south. Along the same line, *Chester et al.* [1991] reported that mineral dust concentrations decreased from a range of 15–20 $\mu g\ m^{-3}$ in the north to a range of 0.01–0.25 $\mu g\ m^{-3}$ below 35°S in the far Southern Ocean. In an earlier study, *Chester et al.* [1985] concluded that the close correspondence between the clay mineralogies of the sediments and dusts in the northern Arabian Sea provided strong evidence for the dominance of the atmospheric pathway for deposition of land-derived material to the sediment surface. *Rhoads et al.* [1997] studied the chemical composition of the troposphere over the Indian Ocean during the monsoonal transition, from March to April 1995. They found that in crossing the ITCZ from south to north, anthropogenic gaseous and particulate matter increased by a factor of 4 due to direct transport of anthropogenic emissions over the Indian Ocean. In 1995, during the U.S. JGOFS project, *Tindale and Pease* [1999] found varying dust concentrations from 0.3 to 180 $\mu g\ m^{-3}$ throughout the year, while during INDOEX 1999 (January to March 1999) the average dry mass concentration in the atmosphere was $\sim$27 $\mu g\ m^{-3}$ [*Lelieveld et al.*, 2001].

[6] The present study in conjunction with our previous observations, which were made in 1995 [*Johansen et al.*, 1999; *Siefert et al.*, 1999], clarify some aspects of the large seasonal differences that exist in the chemistry of the atmosphere over the Arabian Sea. We are primarily interested in the abundance and speciation of Fe as it is thought to be the limiting nutrient for phytoplankton growth in many regions of the open oceans [*Cooper et al.*, 1996; *Kolber et al.*, 1994; *Martin et al.*, 1994; *Martin and Fitzwater*, 1988; *Paerl et al.*, 1994; *Price et al.*, 1994]. As these organisms in turn modulate the biogeochemical cycling of carbon, nitrogen, and sulfur gases between the oceans and the atmosphere, the availability of their micronutrient supply is directly impacting the rates of ocean-atmospheric gas exchange, which are fundamental players in greenhouse warming. Fe(II) is far more soluble than Fe(III), and therefore believed to be more bioavailable. Thus the relative partitioning of aerosol iron between Fe(II) and Fe(III) is a core piece of information needed to make quantitative estimates on the impact of increased iron supply to the open ocean. Reviews by *Wells et al.* [1995] and *Jickells and Spokes* [2001] state that the physico-chemical forms of iron in seawater are not yet well known. Thus, identifying the mechanisms which control the speciation of iron in the atmosphere, which is an important pathway for metals to enter the oceans, would aid our understanding of water column speciation. Detailed reviews on iron speciation in the atmosphere of marine environments were provided by *Johansen et al.* [2000] and *Siefert et al.* [1999]. To our knowledge, the observations of ferrous iron, presented by *Siefert et al.* [1999] and in the present paper, are the first measurements of their kind for aerosol over the Arabian Sea.

2. Experimental

2.1. Sampling Location and Period

[7] Atmospheric aerosol samples were collected over the Arabian Sea during the month of March of 1997. Sampling took place on board the German Research Vessel *Sonne*, which sailed as part of the German Joint Global Ocean Flux Study (JGOFS) project. The cruise track, from Cochin/India to Muscat/Oman, is delineated in the air mass back trajectory plots in Figure 1. Back-trajectory calculations were obtained from the German Weather Service in Hamburg, Germany, based on their isentropic Global-Modell (GME) with a resolution of 190 km [*Deutscher Wetter Dienst*, 1988; *Kottmeier and Fay*, 1998]. In order to get a sense of the vertical motion of the atmosphere, each plot traces five different trajectories which correspond to different initial pressures (i.e., elevations) at the initial position. The highest trajectory, at 850 hPa, represents an altitude of about 1.5 km. The first part of the cruise was predominated by northeasterly winds, as expected; however, later in the cruise, wind patterns changed such that the typical air mass originated over the Saudi Arabian peninsula and the Middle East, much like conditions encountered during the inter-monsoon of 1995 [*Johansen et al.*, 1999; *Siefert et al.*, 1999].

2.2. Aerosol Collection

[8] Ambient aerosol samples were collected with two different collectors. A high-volume dichotomous virtual impactor (HVDVI) was used for the collection of trace metals in two discrete size fractions ($D_{p,50}$ = 3.0 μm) [*Johansen et al.*, 1999, 2000; *Siefert et al.*, 1999], whereby particles of diameter <3.0 μm will presently be defined as the fine particles and particles >3.0 μm in diameter will be denoted as the large particles. The HVDVI collector was constructed with polycarbonate using nylon screws in order to minimize trace metal contamination. The total flow rate was determined to 335 ± 15 $l\ min^{-1}$. The fine and coarse sample fractions were collected on two acid-cleaned 90-mm diameter Teflon filters (Gelman Zefluor, 1-μm pore size). Total elemental composition, Fe(II) concentrations, and

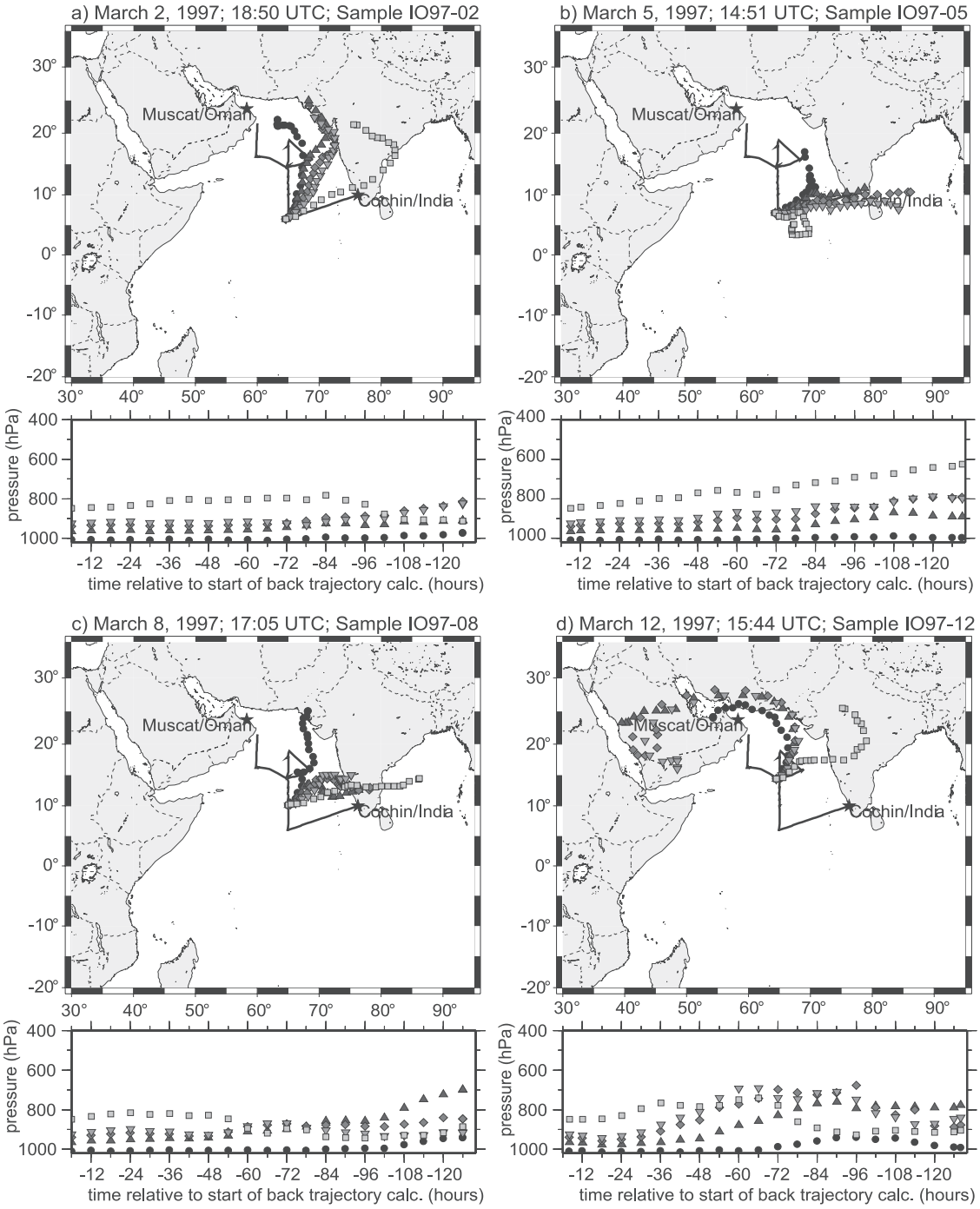

Figure 1. Five-day air mass back trajectory calculations at five different final elevations (based on pressure) above sea level for (a) March 2, 1997; (b) March 5, 1997; (c) March 8, 1997; (d) March 12, 1997; (e) March 18, 1997; (f) March 20, 1997; (g) March 23, 1997; and (h) March 27, 1997.

anion and cation abundances were determined for both fine and coarse filter samples.

[9] Two low-volume collectors, which were operated at flow rates of 27 l min^{-1}, were used for collection of total aerosol mass. Inverted high-density polyethylene bottles (2 L) served as rain shields for the Nucleopore polycarbonate 47-mm-diameter filter holders, which were loaded with acid-cleaned Gelman Zefluor filters (1 μm pore size).

[10] The aerosol collectors and lab equipment were acid cleaned before use by following procedures similar to those outlined by *Patterson and Settle* [1976] employing ultra-pure acids from Seastar Chemicals (Sidney, B.C., Canada) and 18.2 MΩ-cm Milli-Q UV water. After Fe(II) analysis, the remainder of the filters were stored in acid-cleaned polystyrene petri dishes taped shut with Teflon tape, placed inside two plastic bags inside of a plastic container, and stored in a refrigerator during the cruise.

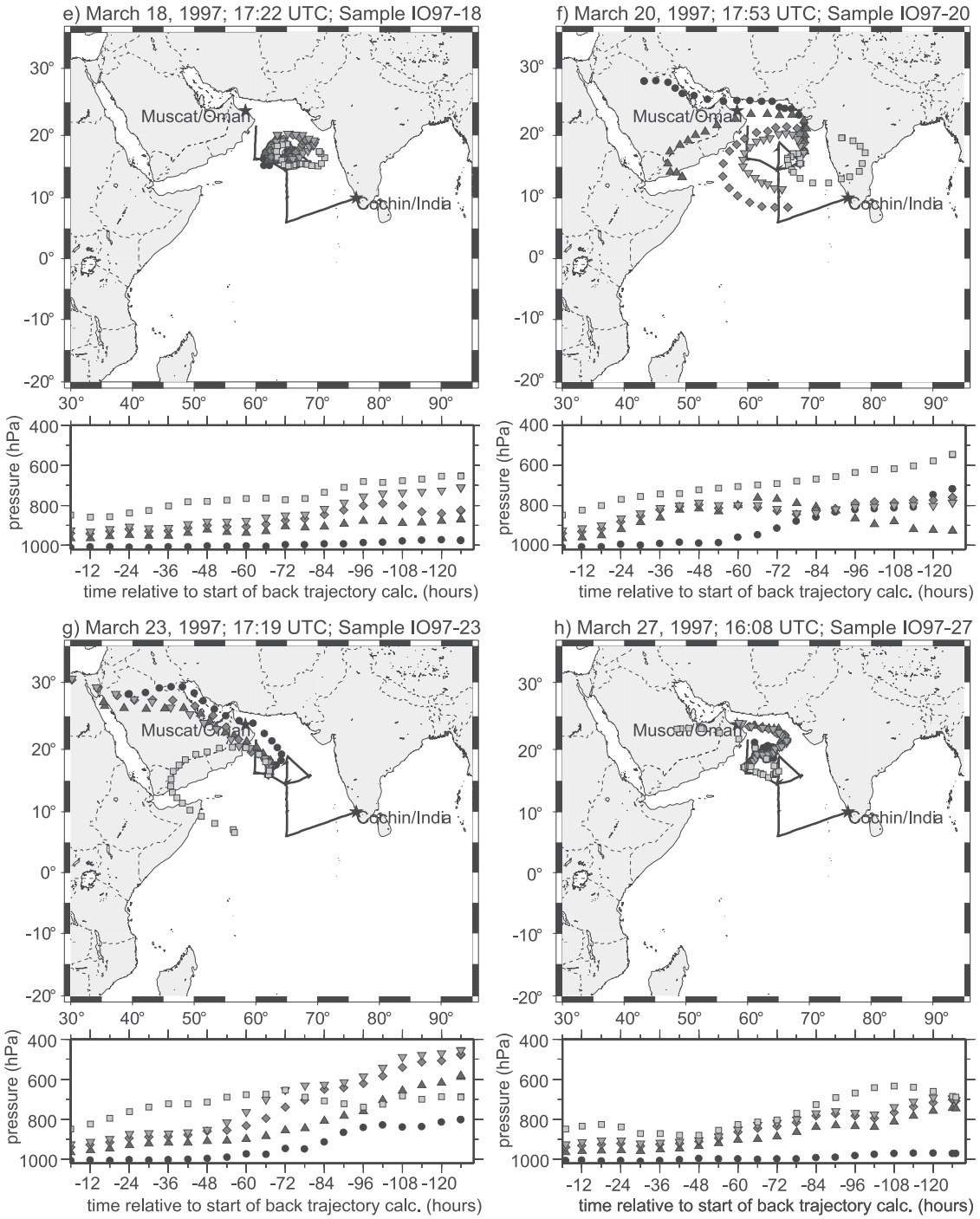

Figure 1. (continued)

After the cruise, the filters were sent back to Caltech (via air-freight, on dry ice) and stored in a freezer until analysis.

[11] A sector sampling system (by Campbell Scientific) controlled the operation of all collector pumps, thereby stopping collection of the aerosol collectors simultaneously when wind speed or wind direction were out of the defined sector. The data logger (CR10, Campbell Scientific) was programmed to shut the pumps off when the wind speed was ≤ 0.2 m s^{-1} and when the relative wind direction was more than $\pm 60^{\circ}$ off of the bow of the ship. In general, collected samples represent daily averages, but due to the ship's cruise track, actual sampling duration may vary slightly.

2.3. Chemical Analyses

2.3.1. Fe(II) Analysis Performed on Board the Ship

[12] Labile Fe(II) in both particle fractions was determined by sequential extraction. These measurements were initiated immediately (within 1 hour) after sample collection in order to minimize the oxidation of Fe(II) to Fe(III). Extraction and quantification procedures are described in

detail by *Siefert et al.* [1999]. Three labile fractions of Fe(II) were determined in each size fraction. The first portion of Fe(II) was released into a 4.2 pH formate buffer after 30 min of leaching; this portion is denoted as aqueous-Fe(II) ($Fe(II)_{aq}$). Thereafter, ferrozine was added to the leaching solution containing the filter, and an absorption reading was made after 5 min. The additional Fe(II) released during this step is the 5-min-ferrozine-Fe(II) ($Fe(II)_{5minFZ}$). The last absorption reading was taken after the ferrozine was in contact with the aerosol for 22 hours (22-hour-ferrozine-Fe(II) ($Fe(II)_{22hrFZ}$)). The total of all three Fe(II) fractions determined in the sequential fashion is defined as total-22-hour-Fe(II) ($Fe(II)_{total,22hourFZ}$). However, owing to the increased potential bias introduced by ferrozine which can reduce Fe(III) over time, it appears more accurate to define a labile Fe(II) fraction that is composed of the first two extractable portions only, thus excluding the 22-hour reading. This total-5-min-FZ-Fe(II) ($Fe(II)_{total,5minFZ}$) will be used when discussing the amount of Fe(II) leached out of the aerosol material. Although the $Fe(II)_{22hrFZ}$ fraction may be biased, it will be discussed briefly because of the very distinct patterns exhibited between the two size fractions. Sample IO97-27 was not analyzed for Fe(II) due to early dismantling of laboratory equipment on the ship.

2.3.2. Elemental Analysis

[13] Elemental analysis of 32 elements (Na, Mg, Al, K, Ca, Sc, Ti, V, Cr, Mn, Fe, Ni, Cu, Zn, Ga, Ge, As, Se, Mo, Ru, Cd, Sn, Sb, Cs, Ba, La, Ce, Sm, Eu, Hf, Pb, and Th) was performed on the high-volume filters with an HP 4500 Inductively Coupled Mass Spectrometer (ICP-MS). The filter digestion technique was presented by *Siefert et al.* [1999] and includes overnight shaking of a filter section in equal amounts of concentrated HNO_3 and HF (from Seastar Chemicals Inc.) at 50°C, and subsequent evaporation to dryness in N_2 atmosphere followed by redissolution in concentrated HNO_3 and dilution with water.

2.3.3. Ion Analysis

[14] For the ion analyses, a small section of the high-volume filter was first wetted with approximately 0.1 mL ethanol, then extracted overnight in 10 mL MQ water. Anions were separated and quantified with a Dionex Bio LC Ion Chromatograph (IC) using an IonPac AS11 separator column and the corresponding AG11 guard column. Organic and inorganic anions were eluted with a gradient pump and a combination of four eluents (5 mM NaOH, 100 mM NaOH, 100% MeOH, MQ H_2O) whereby the NaOH concentration was ramped from an initial 0.45 mM to a final 34.25 mM. The quantified anions included methanesulfonate (MSA), chloride, nitrate, and sulfate. Fluoride, acetate, glycolate, formate, nitrite, bromide, and oxalate were present at very low concentrations that were near the corresponding detection limits. Owing to problems with the IC, three samples were not run correctly (fine IO97-08, fine IO97-18, and coarse IO97-19). The missing data are clearly indicated in the plots, and the samples are removed from the data set when performing statistical analyses.

[15] Cations were separated and quantified isocratically with a DX 500 Ion Chromatograph (IC) with IonPac CS12/CG12 analytical and guard columns and a 20-mM MSA eluent. Sodium, ammonium, potassium, magnesium, and calcium concentrations were determined. Except for NSS-SO_4^{2-}, MSA, Na^+, Mg^{2+}, K^+, and Ca^{2+}, which are included in the principal component analysis, ions will be discussed in a separate study.

3. Results and Discussion

3.1. Air Mass Origins and Characteristics

[16] Air mass back trajectories for a number of samples are plotted in Figure 1. The beginning of the cruise was characterized by air masses that originate from the Indian subcontinent. The different air circulation patterns observed during this period are depicted in Figures 1a, 1b, and 1c, which are representative of the group of samples from IO97-01 to IO97-10. Trajectories in sample IO97-11 (not shown) appear to be transitional between the first and the second group of samples, the latter of which includes samples IO97-12 through IO97-27. The distinguishing characteristic in trajectory pattern between the two groups is the main source of the air masses. As observed in Figures 1d, 1e, 1f, 1g, and 1h, the air masses were swept around in a clockwise manner from the Saudi Arabian peninsula, thus most likely transporting mineral dust from the arid regions of Saudi Arabia to the middle of the Arabian Sea from an apparently northeasterly direction at the collection point. Thus the wind direction observed on board the ship would have erroneously suggested air mass origins in India and Pakistan. Since air mass origins during this second group of samples are similar to those expected during the inter-monsoon [*Johansen et al.*, 1999; *Siefert et al.*, 1999], it is appropriate to report average data from both groups of samples when discussing distinctions between the different monsoon seasons.

[17] Within the second group of samples, air masses vary considerably in their relative transport speeds. Samples IO97-11 through IO97-15 and IO97-20 through IO97-26 (Figures 1d, 1f, and 1g) are representative of air masses that have traveled from the Saudi Arabian peninsula over considerable distances in a relatively short period of time and are, therefore, expected to carry relatively more crustal material compared to air masses sampled in samples IO97-16 through IO97-19 (Figure 1e) and sample IO97-27 (Figure 1h), during which wind speeds were lower.

3.2. Chemical Makeup of Aerosol

[18] Of the 33 elements detected by ICP-MS, the concentrations for elements As, Ru, Cd, Cs, and Sb were found to be below their detection limits and are, therefore, excluded from further discussion. Furthermore, principal component (PC) analyses [*Johansen et al.*, 2000; *Siefert et al.*, 1999] have shown high background concentrations for Cr, Ni, Cu, Mo, and Sn that seem to be attributable to artifacts introduced by the filter material and/or the acids used for the elemental extraction.

[19] Average values for the remaining 22 elements in the coarse and fine fractions for the two groups of atmospheric conditions are listed in Table 1. In order to examine the similarities among these elements and to investigate Fe(II), a PC analysis was performed on 11 of the trace metals in addition to Fe(II) and some anions and cations. The results are presented in Table 2. Four samples (IO97-08, IO97-18, IO97-19, and IO97-27) had to be excluded in this analysis because of miscellaneous data gaps in the anions and Fe(II) concentrations (vide supra).

Table 1. Average, Minimum, and Maximum Atmospheric Trace Metal Concentrations in Coarse and Fine Aerosol for Group 1 and Group 2 Samples[a]

	Group 1 (IO97_01-IO97_10)			Group 2 (IO97_11-IO97_27)		
Element	Average ± SD	Min.	Max.	Average ± SD	Min.	Max.
Na-coarse, μg m^{-3}	0.39 ± 0.14	0.20	0.61	0.49 ± 0.24	0.14	0.88
Na-fine, μg m^{-3}	0.21 ± 0.05	0.13	0.29	0.26 ± 0.13	0.09	0.61
Mg-coarse, μg m^{-3}	0.13 ± 0.06	0.07	0.23	0.16 ± 0.09	0.06	0.38
Mg-fine, μg m^{-3}	0.07 ± 0.02	0.05	0.11	0.10 ± 0.04	0.06	0.21
Al-coarse, μg m^{-3}	0.32 ± 0.13	0.16	0.56	0.30 ± 0.24	0.08	0.93
Al-fine, μg m^{-3}	0.15 ± 0.03	0.10	0.21	0.21 ± 0.09	0.11	0.04
K-coarse, μg m^{-3}	0.05 ± 0.04	0.01	0.15	0.10 ± 0.09	0.02	0.35
K-fine, μg m^{-3}	0.19 ± 0.06	0.09	0.30	0.15 ± 0.09	0.04	0.38
Ca-coarse, μg m^{-3}	0.31 ± 0.17	0.13	0.60	0.38 ± 0.19	0.13	0.74
Ca-fine, μg m^{-3}	0.12 ± 0.04	0.08	0.20	0.17 ± 0.9	0.09	0.39
Sc-coarse	0.083 ± 0.036	0.038	0.142	0.070 ± 0.058	0.022	0.230
Sc-fine	0.039 ± 0.007	0.027	0.053	0.047 ± 0.017	0.027	0.094
Ti-coarse	25.99 ± 10.90	13.57	45.14	24.02 ± 16.42	5.90	64.80
Ti-fine	11.85 ± 1.98	8.21	14.74	16.82 ± 6.83	10.04	32.39
V-coarse	0.73 ± 0.30	0.36	1.25	0.69 ± 0.48	0.18	1.92
V-fine	1.18 ± 0.16	0.86	1.38	1.19 ± 0.42	0.50	1.98
Mn-coarse	6.48 ± 2.57	3.70	10.37	5.09 ± 2.55	1.43	10.52
Mn-fine	4.69 ± 1.22	3.34	6.38	5.26 ± 2.28	2.29	9.40
Fe-coarse, μg m^{-3}	0.39 ± 0.20	0.19	0.89	0.31 ± 0.17	0.08	0.70
Fe-fine, μg m^{-3}	0.33 ± 0.13	0.17	0.53	0.41 ± 0.25	0.15	0.89
Zn-coarse	1.95 ± 0.44	1.29	2.63	0.99 ± 0.49	0.30	1.83
Zn-fine	9.72 ± 3.68	5.56	17.32	3.98 ± 2.15	1.55	9.16
Ga-coarse	0.14 ± 0.05	0.07	0.24	0.12 ± 0.07	0.03	0.28
Ga-fine	0.08 ± 0.01	0.06	0.10	0.09 ± 0.03	0.05	0.17
Ge-coarse	0.027 ± 0.008	0.027	0.039	0.021 ± 0.010	0.007	0.045
Ge-fine	0.045 ± 0.013	0.026	0.066	0.032 ± 0.010	0.017	0.050
Se-coarse	0.081 ± 0.030	0.036	0.137	0.069 ± 0.036	0.036	0.142
Se-fine	0.306 ± 0.094	0.214	0.514	0.257 ± 0.100	0.113	0.490
Ba-coarse	2.19 ± 0.81	1.12	3.64	1.64 ± 0.89	0.47	3.56
Ba-fine	1.01 ± 0.16	0.66	1.29	1.18 ± 0.42	0.62	2.27
La-coarse	0.17 ± 0.06	0.08	0.27	0.14 ± 0.10	0.04	0.40
La-fine	0.09 ± 0.1	0.06	0.11	0.11 ± 0.04	0.06	0.23
Ce-coarse	0.36 ± 0.14	0.18	0.59	0.33 ± 0.23	0.08	0.89
Ce-fine	0.18 ± 0.03	0.12	0.24	0.24 ± 0.10	0.13	0.48
Sm-coarse	0.031 ± 0.012	0.015	0.049	0.026 ± 0.017	0.008	0.067
Sm-fine	0.015 ± 0.003	0.009	0.019	0.018 ± 0.006	0.011	0.033
Eu-coarse	0.0078 ± 0.0028	0.0045	0.0123	0.0056 ± 0.0035	0.0018	0.0149
Eu-fine	0.0034 ± 0.0004	0.0028	0.0041	0.0043 ± 0.0013	0.0027	0.0069
Hf-coarse	0.020 ± 0.008	0.010	0.033	0.022 ± 0.010	0.010	0.039
Hf-fine	0.011 ± 0.003	0.008	0.016	0.021 ± 0.009	0.009	0.041
Pb-coarse	0.80 ± 0.18	0.52	1.09	0.39 ± 0.18	0.02	0.65
Pb-fine	6.78 ± 1.82	4.67	10.46	3.52 ± 1.70	1.32	6.88
Th-coarse	0.052 ± 0.020	0.023	0.088	0.047 ± 0.39	0.012	0.149
Th-fine	0.024 ± 0.004	0.015	0.032	0.031 ± 0.014	0.016	0.071

[a]Concentrations in ng m^{-3} unless otherwise noted.

[20] The first eight components of this analysis carry eigenvalues larger than 1 and account for a cumulative variance of 90.3% of the data set. The variance described by each component appears across the top of the table.

[21] The first component, which is representative of a crustal source, has relatively "large" (i.e., values close to 1) values for typical crustal material tracers, such as Al and Sc (as well as Ti, Ba, La, Ce, Sm, Eu, and Th, not shown). No other known sources exist for these elements, therefore, they can be used reliably as indicators of crustal material. Some of the other elements (K, V, Mn, and Fe) that can be associated with gas-to-particle reactions of anthropogenic pollutants from combustion sources may still display crustal characteristics in the coarse fraction since gas-to-particle reactions result in fine particles. Concentrations for the crustal tracer Al are plotted as a function of sample ID in Figure 2a. For comparison, the factor scores for the crustal component (PC 1) are plotted in Figure 3a. As expected, the two variables trace each other closely.

[22] The second component in the PC analysis reflects an anthropogenic source, typified by Pb and Zn in both size fractions (and Ge and Se, not shown) as well as K in the fine fraction. While Pb and Zn reach the atmosphere through burning of fossil fuel and smelting operations, respectively, K is a product of biomass burning and waste incinerators [*Andreae*, 1983; *Echalar et al.*, 1995; *Fishman et al.*, 1999]. Figure 2b presents the coarse and fine Pb concentrations in stacked bars as a function of sample ID. The plots for Pb, Zn, and K (latter two not shown) are all similar, and as expected for anthropogenic tracers, their concentrations are larger in the fine fraction as compared to the coarse fraction. The geometric mean for the relative abundance of Pb in the fine fraction is 89 ± 3%, for Zn it is 80 ± 8%, and for K it is 67 ± 16%. Factor scores for PC 2 in Figure 3a carry the same fingerprint as Pb. Consistent with our observations of the air mass back trajectories, PC 2 is predominant in samples of group 1, which are characteristic of the northeast monsoon. Lead and zinc concen-

Table 2. Varimax Rotated Principal Component Matrix[a]

Element\Component	1 Crustal (24.6%)	2 Anthrop. (19.4%)	3 Crustal High in Ca and Mg (14.2%)	4 Sea Salt (11.3%)	5 Fe(II)-fine (6.2%)	6 MSA, NSS-SO_4^{2-} coarse (5.8%)	7 Fe, Mn-fine (4.8%)	8 (3.9%)
Na-coarse	0.263	−0.025	0.096	**(0.913)**	−0.111	−0.140	−0.132	0.029
Na-fine	0.192	0.181	0.390	**(0.648)**	−0.277	0.219	−0.079	0.306
Mg-coarse	**(0.894)**	−0.246	0.158	0.245	0.058	0.042	0.131	−0.035
Mg-fine	0.433	−0.197	**(0.786)**	0.077	−0.048	0.230	0.119	0.250
Al-coarse	**(0.962)**	−0.002	−0.016	0.069	0.140	0.090	0.143	−0.008
Al-fine	**(0.661)**	−0.206	**(0.528)**	−0.086	−0.022	0.206	0.152	0.367
K-coarse	**(0.866)**	−0.201	0.141	0.257	0.212	0.093	0.140	0.138
K-fine	0.219	**(0.835)**	−0.012	0.148	0.187	0.047	0.003	0.348
Ca-coarse	**(0.704)**	−0.202	0.469	0.160	0.009	−0.027	0.124	−0.336
Ca-fine	0.076	−0.080	**(0.958)**	0.069	−0.073	0.128	0.134	0.036
Sc-coarse	**(0.945)**	0.018	−0.098	0.055	0.079	0.098	0.161	−0.090
Sc-fine	**(0.595)**	−0.137	0.462	−0.370	−0.114	0.247	0.066	0.200
V-coarse	**(0.938)**	0.068	0.079	0.167	0.204	0.121	0.096	−0.002
V-fine	0.373	0.411	0.059	0.040	0.441	0.229	0.173	0.408
Mn-coarse	**(0.875)**	0.259	0.105	0.059	0.103	0.038	−0.244	−0.064
Mn-fine	0.276	0.092	0.459	−0.129	0.205	0.225	**(0.714)**	0.068
Fe-coarse	**(0.758)**	0.129	0.073	−0.036	0.070	−0.028	−0.344	0.027
Fe-fine	0.167	−0.074	0.347	−0.194	0.216	0.194	**(0.786)**	−0.037
Zn-coarse	0.410	**(0.650)**	−0.212	0.038	0.214	0.154	−0.190	−0.152
Zn-fine	−0.079	**(0.933)**	−0.188	−0.016	−0.024	0.100	0.004	−0.021
Pb-coarse	0.318	**(0.794)**	−0.098	0.082	0.174	−0.077	−0.190	−0.231
Pb-fine	−0.039	**(0.962)**	0.015	0.087	−0.080	0.054	−0.020	−0.061
FeII-$coarse_{total,22hrsFZ}$	**(0.604)**	**(0.562)**	0.164	0.180	−0.113	0.269	0.171	−0.158
FeII-$fine_{total,22hrsFZ}$	0.311	0.313	0.383	−0.111	**(0.706)**	0.205	0.131	−0.012
FeII-$coarse_{total,5minFZ}$	**(0.772)**	0.245	0.171	0.020	−0.215	0.283	−0.026	0.232
FeII-$fine_{total,5minFZ}$	0.209	0.339	−0.002	−0.206	**(0.797)**	0.169	0.209	−0.053
Na^+-coarse	0.005	0.045	0.011	**(0.963)**	−0.037	0.002	0.074	−0.130
Na^+-fine	0.029	0.186	0.251	**(0.673)**	0.224	0.119	−0.297	0.068
Mg^{2+}-coarse	0.456	0.053	0.074	**(0.820)**	−0.024	0.185	−0.033	0.020
Mg^{2+}-fine	0.109	−0.019	**(0.622)**	0.437	**(0.547)**	0.057	−0.041	0.130
K^+-coarse	−0.027	**(0.671)**	−0.168	**(0.638)**	−0.196	0.047	0.078	0.076
K^+-fine	−0.211	**(0.856)**	−0.158	0.009	0.315	−0.172	−0.051	0.141
NSS-K^+-coarse	−0.038	**(0.822)**	−0.220	0.203	−0.224	0.060	0.052	0.178
NSS-K^+-fine	−0.216	**(0.852)**	−0.178	−0.040	0.304	−0.185	−0.032	0.138
Ca^{2+}-coarse	**(0.663)**	−0.246	0.463	0.190	0.017	0.370	0.154	−0.199
Ca^{2+}-fine	0.071	−0.212	**(0.935)**	0.147	0.151	0.021	0.098	−0.037
NSS-Ca^{2+}-coarse	**(0.668)**	−0.249	0.466	0.149	0.019	0.373	0.153	−0.194
NSS-Ca^{2+}-fine	0.070	−0.230	**(0.934)**	0.099	0.138	0.009	0.124	−0.043
NSS-SO_4^{2}-coarse	0.227	0.202	0.239	0.058	0.148	**(0.773)**	0.222	−0.197
NSS-SO_4^{2}-fine	−0.269	**(0.832)**	−0.044	−0.097	0.269	−0.094	0.059	−0.291
MSA-coarse	0.299	−0.144	0.139	0.075	0.168	**(0.823)**	0.062	0.155
MSA-fine	0.314	0.245	−0.333	0.316	0.201	0.253	−0.353	−0.348
Wind speed	−0.461	0.096	0.188	**(0.418)**	0.066	−0.248	−0.065	**(0.536)**

[a]Variance is given in parentheses in each heading. Rotation converged in nine iterations. Data set includes 23 samples. All components have eigenvalues >1 and account for a cumulative variance of 90.3%.

trations increase by factors of 2.2 and 2.3, respectively, between samples of group 1 and 2.

[23] The third component (PC 3) represents another crustal source, rich in Ca and Mg. Upon inspection of its factor scores in Figure 3b, it is evident that this crustal component becomes of importance during the latter part of samples in the second group, especially in samples IO97-20 and IO97-24. Air mass back trajectories in Figure 1 indicate that these air masses were transported with relatively greater wind speeds from the Saudi Arabian Peninsula and as far as northeastern Africa. The apparently distinct chemical signatures between the two crustal components may also be a function of aerosol particle size and the different chemical transformations occurring during transport. Owing to the large correlation of PC 3 with the water soluble fractions of Ca and Mg (Ca^{2+} and Mg^{2+} in Table 2), it is likely that this crustal component carries a gypsum, calcite, and/or limestone fraction, all of which are typical constituents of clay minerals. A clay mineralogical study of the aerosol material over the Arabian Sea [*Chester et al.*, 1985] revealed that illite is the dominant clay mineral. Illite was also observed to be the predominant clay mineral in most sediments from the northern Arabian Sea [*Goldberg and Griffin*, 1970].

[24] The fourth principal component (PC 4) is representative of the sea salt, and its factor scores are plotted in Figure 3b. Water-soluble Na (Na^+, in Table 2) is used as the primary sea-salt tracer; however, Na, as plotted in Figure 2d, can potentially include a crustal source because it was determined by ICP-MS on a section of acid leached filter material. Within the analytical errors of our techniques, however, the crustal Na was negligible. The sea-salt component usually correlates well with the wind speed due to the increased wave action on the water surface, which leads to sea-salt aerosol formation; however, due to the relatively low wind speeds encountered during the present cruise, this correlation is only weak.

[25] PC 5 and PC 6 will be discussed below in conjunction with iron speciation. Fe and Mn in the fine fractions correlate with each other in PC 7. The source of fine Fe and Mn could arise from local incinerators or even from our research

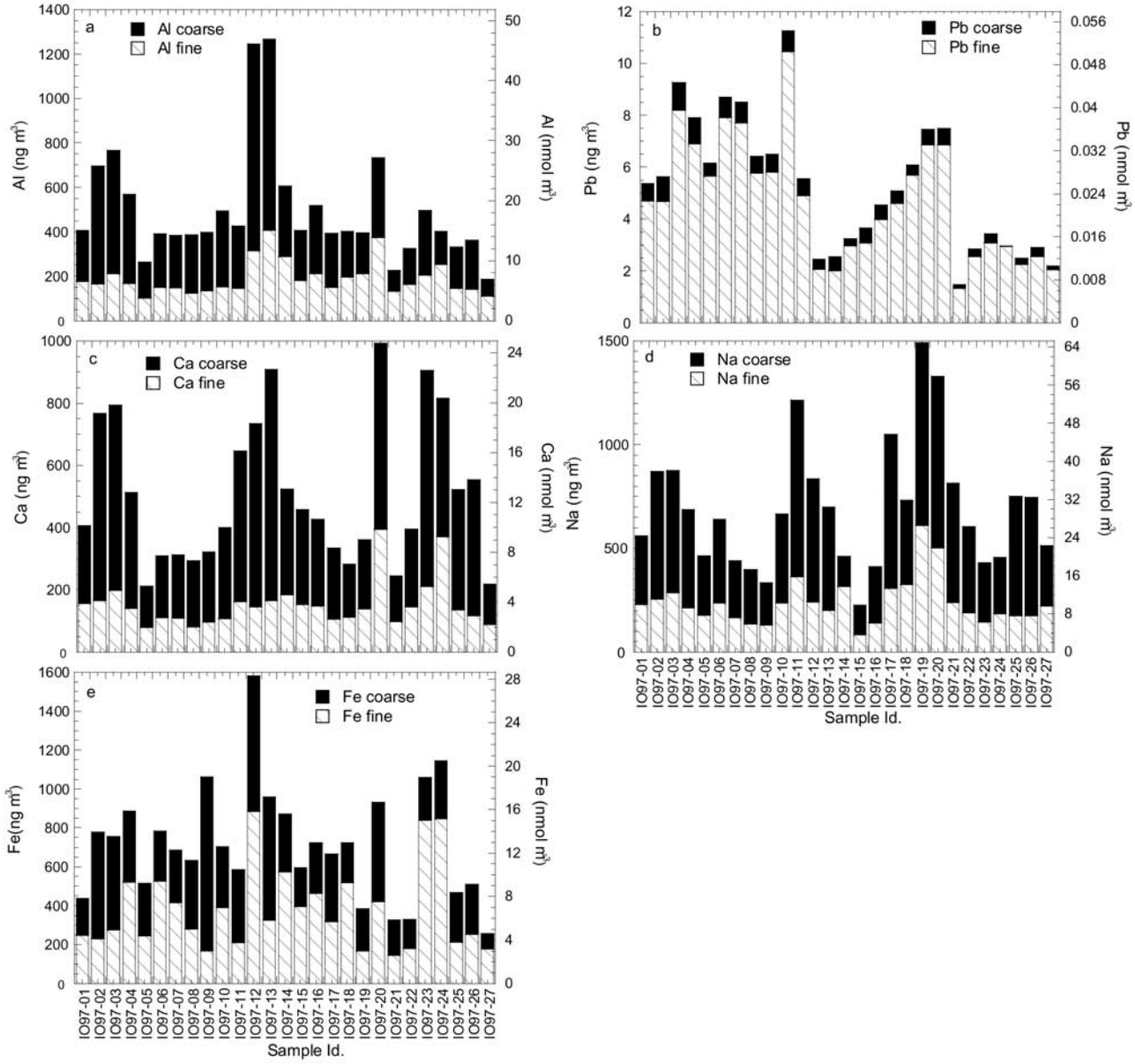

Figure 2. Coarse and fine fraction trace metal concentrations versus sample ID. for (a) Al, (b) Pb, (c) Ca, (d) Na, and (e) Fe.

vessel's smoke stack. The same elements were observed to be enriched during a previous cruise on the R/V *Meteor* [*Siefert et al.*, 1999]. Since both these vessels use diesel fuel and electric power generators to propel the ship, V was not expected to be seen in the ship's plume [*Hopke*, 1985]. However, Fe and Mn during the *Meteor* cruise were enriched in collected samples when the sampling sector system was malfunctioning. Thus there is a slight chance that although the sector sampling system was working well during the whole present cruise, minute amounts of the ship's plume may have reached the sampling setup during the ship's maneuvers. Fe concentrations are plotted in Figure 2e. The eighth component was retained in Table 2 but does not have any physical meaning other than that it seems to be slightly representative of the wind speed.

[26] As with the inter-monsoon samples collected in 1995 [*Johansen et al.*, 1999], the crustal average according to *Taylor and McLennan* [1985] appears to adequately represent the sampled mineral dust; however, an additional crustal Ca source seems present in all the samples. On the basis of the crustal average and the observed Al concentrations, the mineral dust concentrations averaged 5.7 ± 1.7 μg m^{-3} (67.8% in the coarse fraction) during the first group of samples and 6.1 ± 3.6 μg m^{-3} (58.4% in the coarse fraction) for the second group of samples. These two average crustal masses do not prove to be statistically different, thus indicating that the crustal component during the northeast monsoon and inter-monsoon may be of comparable magnitude. During the inter-monsoon of 1995, *Johansen et al.* [1999] observed a very similar crustal average of 5.85 ± 4.24 μg m^{-3}, while during the southwest monsoon, concentrations were considerably lower, 0.66 ± 0.43 μg m^{-3}. *Rhoads et al.* [1997] found very similar values of 6.2 ± 4.4 μg m^{-3} during the months of March and April

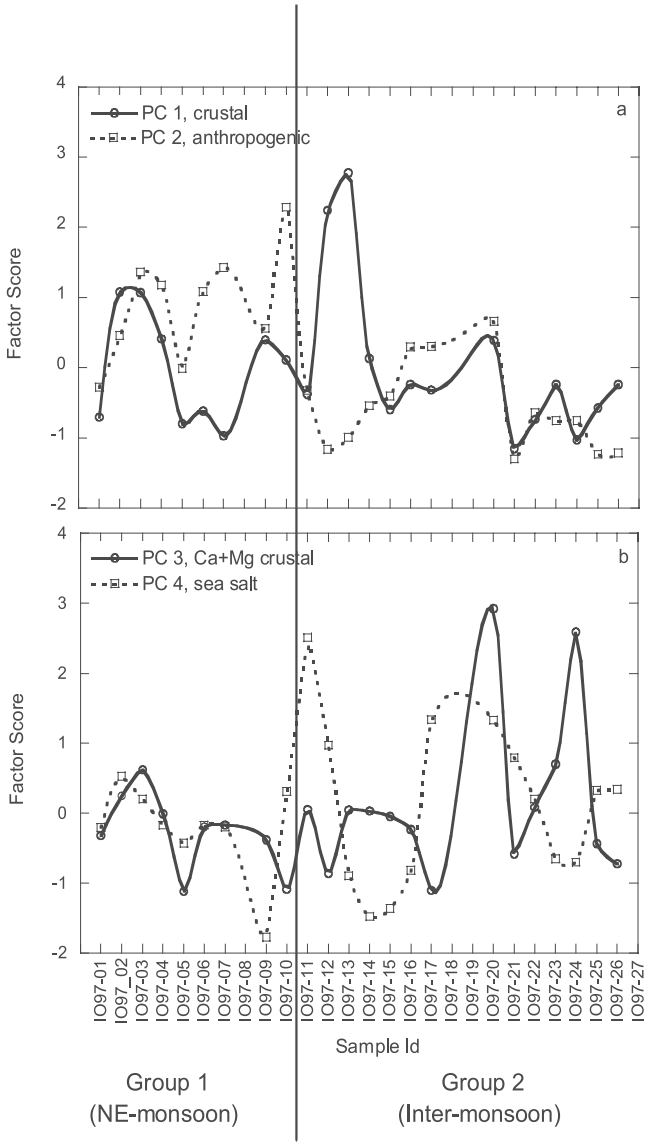

Figure 3. Factor scores for (a) the first three and (b) the second three principal components extracted in the principal component analysis in Table 2.

of 1995. *Chester et al.* [1991] reported mineral dust concentrations decreasing from 15–20 μg m^{-3} in the north to 0.01–0.25 μg m^{-3} below 35°S in the far Southern Ocean. *Pease et al.* [1998] obtained mineral dust concentrations of 40 μg m^{-3} during the northeast monsoon of 1995, while *Savoie et al.* [1987] measured dust concentrations of only 1.01 ± 0.81 μg m^{-3} during the northeast monsoon of 1979.

3.3. Fe and Fe(II)

[27] The PC analysis in Table 2 shows that coarse Fe seems to be of crustal origin (PC 1), while most of the fine Fe, which is comparable in magnitude to the mass in the coarse Fe, correlates with fine Mn (PC 7) for which the source is not obvious. On the basis of enrichment factor analysis (not shown), fine iron is on average 2.4 times the value expected from the crustal contribution, whereby there is no statistical difference between the group 1 and group 2 samples.

[28] Ferrous iron in the coarse fraction seems to be crustal derived (PC 1), while ferrous iron in the fine fraction (PC 5) does not correlate with any component but itself. The implications are that Fe(II) in the fine fraction must be regulated by either one or more unknown parameters in addition to a combination of the existing parameters. Assuming that the concentrations of all other pH modulating constituents in the aerosol particle remain unchanged, the biological NSS-SO_4^{2-} contribution should lead to an acidification of the aerosol. However, from this study it is not clear that the biogenically derived NSS-SO_4^{2-} acidity influences the concentration of Fe(II), as proposed by *Zhuang et al.* [1992] and indicated by *Johansen et al.* [2000].

[29] The three extracted Fe(II) portions for both coarse and fine fractions are presented in stacked bar plots in Figures 4a and 4b, respectively. Superimposed, in dashed

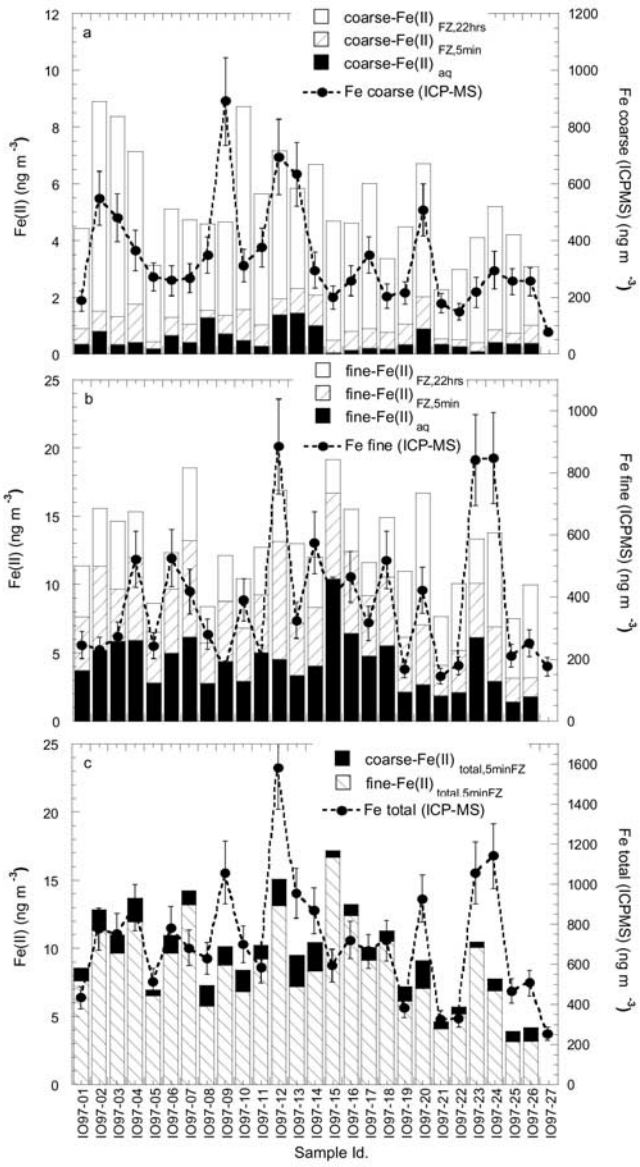

Figure 4. Fe(II) concentrations versus sample ID. (a) Fe(II) in the coarse fraction, (b) Fe(II) in the fine fraction, and (c) total Fe(II) released after 5 min in ferrozine (see text for details).

lines, are the corresponding Fe concentrations determined by ICP-MS.

[30] Although, as mentioned earlier, there is an increased possibility of ferrozine reacting with Fe during the 22-hour extraction experiment, it is peculiar that the coarse and fine fractions exhibit widely different behaviors with regard to the amount of Fe(II) released in the three consecutive extraction steps. In the coarse fraction the $Fe(II)_{22hrFZ}$ (white columns in Figure 4a) comprised 80% of all released Fe(II) while the $Fe(II)_{5minFZ}$ and $Fe(II)_{aq}$ made up ~10% each. In the fine fraction all components of labile Fe(II) were equal in magnitude within the experimental uncertainty. This result may be a function of the surface area of the particles, the mineralogical composition of the phases present, and/or the presence of species which may reduce Fe(III) to Fe(II) over the course of the 22-hour extraction experiment.

[31] Coarse- and fine-$Fe(II)_{total,5minFZ}$ are plotted in Figure 4c in stacked bars, together with the total Fe concentration. No statistical difference could be detected between the group 1 and group 2 Fe(II) data. Figure 4c shows that most (87.2 ± 6.1%) of the $Fe(II)_{total,5minFZ}$, which averages 9.76 ± 3.37 ng m^{-3}, is present in the fine fraction. Compared to the total Fe as determined by ICP-MS, the combined coarse and fine $Fe(II)_{total,5minFZ}$ account for only 1.3 ± 0.5% (geometric mean), ranging from 0.7 to 2.9%. The average coarse-$Fe(II)_{total,5minFZ}$ concentration of 1.16 ± 0.55 ng m^{-3} amounts to 0.3 ± 0.1% (geometric mean) of the coarse Fe, whereby the fine-$Fe(II)_{total,5minFZ}$ concentration of 8.60 ± 3.29 ng m^{-3}, amounts to 2.4 ± 1.2% (geometric mean) of the fine Fe. As mentioned earlier, note that total Fe is almost evenly distributed between the fine (52.8%) and the coarse (47.2%) fractions.

[32] Compared to previous observations reported by our group, the present samples show relative Fe(II) abundances that are slightly larger. During the inter-monsoon of 1995 [*Siefert et al.*, 1999] an average of 0.3% of the total Fe was observed as Fe(II), whereby the actual combined coarse and fine $Fe(II)_{total,5minFZ}$ amounted to 5.2 ± 4.4 ng m^{-3}. During the Atlantic Ocean cruise [*Johansen et al.*, 2000], the measured $Fe(II)_{total,5minFZ}$ concentrations averaged 3.14 ± 1.35 ng m^{-3}, which accounted for 0.5 ± 0.4% of the total Fe. Thus the $Fe(II)_{total,5minFZ}$ concentrations reported here are larger by a factor of 1.9 and 3.1, respectively, compared to those we previously reported. This observation may be indicative of the anthropogenic constituent playing an indirect but pronounced role in the speciation of iron.

[33] Few studies exist on Fe(II) concentrations measured over remote oceanic regions. *Zhu et al.* [1993, 1997] reported similar concentrations to those found in the present study, while *Zhuang et al.* [1992] measured relative Fe(II) values that were considerably larger (15%, corrected value [see *Zhu et al.*, 1993]) in Barbados. However, these large discrepancies may be due to different sample handling and more vigorous experimental extraction procedures.

4. Conclusions

[34] Air masses sampled during the month of March of 1997 over the Arabian Sea contain aerosols that vary in their mineralogical characteristics. This is expected, since March is considered to be a transitional period between the tail end of the northeast monsoon and inter-monsoon seasons. The mineral aerosol appears to be a composite from several arid and semiarid regions surrounding the Arabian Sea. On the basis of air mass back trajectories the Thar desert and deserts of the Saudi Arabian peninsula are the most likely mineral dust sources. PC analyses reveal two distinct crustal components. The predominant crustal source represents 5.94 ± 3.08 μg m^{-3} of soil material, while the second minor component is enriched in water-soluble Ca^{2+} and Mg^{2+} species, possibly as a form of clay.

[35] All samples carry a strong anthropogenic signature reflected in the large enrichments in anthropogenic tracers such as Pb, Zn, fine K, NSS-K^{+}, and NSS-SO_4^{2-}. The anthropogenic contribution is especially pronounced in the first 10 samples, which exhibit air mass back trajectories that indicate a northeastern origin, from the Indian subcontinent.

[36] Iron in the coarse fraction appears to be of a crustal origin, while the fine fraction Fe correlates with the fine fraction Mn of an unknown component. Ferrous iron concentrations in the coarse fraction correlate with the coarse crustal Fe; however, in the fine fraction, no such simple relationship is observed. Fine plus coarse $Fe(II)_{total,5minFZ}$ averages 9.76 ± 3.37 μg m^{-3}, which represents 1.3 ± 0.5% of the total Fe. These values are the largest observed by our group as compared to measurements taken during other seasons over the Arabian Sea [*Siefert et al.*, 1999] and over the Atlantic Ocean [*Johansen et al.*, 2000]. While total Fe is almost evenly distributed between fine and coarse fractions, 87.2 ± 6.1% of the $Fe(II)_{total,5minFZ}$ is present in the fine fraction. Furthermore, on the basis of the relative amounts of Fe(II) released in the sequential extraction procedure, it appears as if the Fe(II) in the fine fraction is more labile.

[37] **Acknowledgments.** The authors wish to thank Meinrat O. Andreae and Hermann W. Bange of the Max Planck Institute of Biogeochemistry in Mainz, Germany, for assistance with the cruise, which was sponsored by the German Joint Global Ocean Flux Study (JGOFS) project. Appreciation is also extended to the helpful crew of the R/V *Sonne*. Research support was provided by the National Science Foundation and by the Environmental Now Foundation. Their support is greatly appreciated. This paper was abstracted in part from the Ph.D. thesis of A. M. Johansen, California Institute of Technology.

References

Ackerman, A. S., and S. K. Cox, Surface weather observations of atmospheric dust over the southwest summer monsoon region, *Meteorol. Atmos. Phys.*, *41*, 19–34, 1989.

Andreae, M. O., Soot carbon and excess fine potassium: Long-range transport of combustion-derived aerosols, *Science*, *220*, 1148–1151, 1983.

Ansmann, A., D. Althausen, U. Wandinger, K. Franke, D. Muller, F. Wagner, and J. Heintzenberg, Vertical profiling of the Indian aerosol plume with six-wavelength lidar during INDOEX: A first case study, *Geophys. Res. Lett.*, *27*(7), 963–966, 2000.

Chester, R., E. J. Sharples, and G. S. Sanders, The concentrations of particulate aluminum and clay minerals in aerosols from the northern Arabian Sea, *J. Sediment. Petrol.*, *55*(1), 37–41, 1985.

Chester, R., A. S. Berry, and K. J. T. Murphy, The distributions of particulate atmospheric trace metals and mineral aerosols over the Indian Ocean, *Mar. Chem.*, *34*, 261–290, 1991.

Cooper, D. J., A. J. Watson, and P. D. Nightingale, Large decrease in ocean-surface CO_2 fugacity in response to in situ iron fertilization, *Nature*, *383*, 511–514, 1996.

Deutscher Wetter Dienst, Global-Modell (GME), Hamburg, Germany, 1988.

Echalar, F., A. Gaudichet, H. Cachier, and P. Artaxo, Aerosol emissions by tropical forest and savanna biomass burning: Characteristic trace elements and fluxes, *Geophys. Res. Lett.*, *22*(22), 3039–3042, 1995.

Findlater, J., A major low-level air current near the Indian Ocean during the northern summer, *Q.J.R. Meteorol. Soc.*, *95*, 362–380, 1969.

Findlater, J., Mean monthly airflow at low levels over the western Indian Ocean, *Geophys. Mem. London*, *115*(26), 1–53, 1971.

Fishman, N. S., C. A. Rice, G. N. Breit, and R. D. Johnson, Sulfur-bearing coatings in fly ash from a coal-fired power plant: Composition, origin, and influence on ash alteration, *Fuel*, *78*, 187–196, 1999.

Goldberg, E. D., and J. J. Griffin, The sediments of the northern Indian Ocean, *Deep Sea Res.*, *17*, 513–537, 1970.

Hopke, P. K., Appendix: Selected Source Profiles, in *Receptor Modeling in Environmental Chemistry*, pp. 267–314, John Wiley, New York, 1985.

Hoppel, W. A., J. W. Fitzgerald, G. M. Frick, R. E. Larson, and E. J. Mack, Aerosol size distributions and optical properties found in the marine boundary layer over the Atlantic Ocean, *J. Geophys. Res.*, *95*, 3659–3686, 1990.

Jayaraman, A., D. Lubin, S. Ramachandran, V. Ramanathan, E. Woodbridge, W. D. Collins, and K. S. Zalpuri, Direct observations of aerosol radiative forcing over the tropical Indian Ocean during the January–February 1996 pre-INDOEX, *J. Geophys. Res.*, *103*, 13,827–13,836, 1998.

Jickells, T. D., and L. J. Spokes, Atmospheric iron inputs to the oceans, in *The Biogeochemistry of Iron in Seawater*, edited by D. R. Turner and K. A. Hunter, pp. 86–121, John Wiley, New York, 2001.

Johansen, A. M., R. L. Siefert, and M. R. Hoffmann, Chemical characterization of ambient aerosol collected during the southwest-monsoon and inter-monsoon seasons over the Arabian Sea: Anions and cations, *J. Geophys. Res.*, *104*, 26,325–26,347, 1999.

Johansen, A. M., R. L. Siefert, and M. R. Hoffmann, Chemical composition of aerosols collected over the tropical North Atlantic Ocean, *J. Geophys. Res.*, *105*, 15,277–15,312, 2000.

Kolber, Z. S., R. T. Barber, K. H. Coale, S. E. Fitzwater, R. M. Greene, K. S. Johnson, S. Lindley, and P. G. Falkowski, Iron limitation of phytoplankton photosynthesis in the equatorial Pacific Ocean, *Nature*, *371*, 145–149, 1994.

Kottmeier, C., and B. Fay, Trajectories in the Antarctic lower troposphere, *J. Geophys. Res.*, *103*, 10,947–10,959, 1998.

Lelieveld, J., et al., The Indian Ocean Experiment: Widespread air pollution from South and Southeast Asia, *Science*, *291*, 1031–1036, 2001.

Martin, J. H., and S. F. Fitzwater, Iron deficiency limits phytoplankton growth in the north-east Pacific subarctic, *Nature*, *331*, 341–342, 1988.

Martin, J. H., et al., Testing the iron hypothesis in ecosystems of the equatorial Pacific Ocean, *Nature*, *371*, 123–129, 1994.

Middleton, N. J., Dust storms in the Middle East, *J. Arid Environ.*, *10*, 83–96, 1986a.

Middleton, N. J., A geography of dust storms in south-west Asia, *J. Climatol.*, *6*, 183–196, 1986b.

Moorthy, K. K., S. K. Satheesh, and K. B. V. Murthy, Investigations of marine aerosols over the tropical Indian Ocean, *J. Geophys. Res.*, *102*, 18,827–18,842, 1997.

Moorthy, K. K., S. K. Satheesh, and B. V. K. Murthy, Characteristics of spectral optical depth and size distributions of aerosols over tropical oceanic regions, *J. Atmos. Solar Terr. Phys.*, *60*, 981–992, 1998.

Moorthy, K., P. Pillai, A. Saha, and K. Niranjan, Aerosol size characteristics over the Arabian Sea and Indian Ocean: Extensive sub-micron aerosol loading in the Northern Hemisphere, *Curr. Sci.*, *76*, 961–967, 1999.

Moorthy, K., A. Saha, and K. Niranjan, Spatial variation of aerosol spectral optical depth and columnar water vapour content over the Arabian Sea and Indian Ocean during the IFP of INDOEX, *Curr. Sci.*, *80*, 145–150, 2001.

Paerl, H. W., L. E. Prufert-Bebout, and C. Guo, Iron-stimulated N_2 fixation and growth on natural and cultured populations of the planktonic marine cyanobacteria *Trichodesmium* spp., *Appl. Environ. Microbiol.*, *60*(3), 1044–1047, 1994.

Patterson, C. C., and D. M. Settle, The reduction of orders of magnitude errors in lead analysis of biological materials and natural waters by evaluating and controlling the extent and sources of industrial lead contamination introduced during sampling, collecting, handling and analysis, *NBS Spec. Publ. U.S.*, *422*, 321–351, 1976.

Pease, P. P., V. P. Tchakerian, and N. W. Tindale, Aerosols over the Arabian Sea: Geochemistry and source areas for aeolian desert dust, *J. Arid Environ.*, *39*, 477–496, 1998.

Price, N. M., B. A. Ahner, and F. M. M. Morel, The equatorial Pacific Ocean: Grazer-controlled phytoplankton populations in an iron-limited ecosystem, *Limnol. Oceanogr.*, *39*(3), 520–534, 1994.

Rao, P., G. Momin, P. Safai, K. Ali, M. Naik, and A. Pillai, Aerosol and trace gas studies at Pune during INDOEX IFP-99, *Curr. Sci.*, *80*, 105–109, 2001.

Rao, Y., and P. Devara, Characterization of aerosols over Indian Ocean and Arabian Sea during INDOEX IFP-99, *Curr. Sci.*, *80*, 120–122, 2001.

Rhoads, K. P., P. Kelley, R. R. Dickerson, T. P. Carsey, M. Farmer, D. L. Savoie, and J. M. Prospero, Composition of the troposphere over the Indian Ocean during the monsoonal transition, *J. Geophys. Res.*, *102*, 18,981–18,995, 1997.

Satheesh, S. K., and K. Krishna Moorthy, Aerosol characteristics over coastal regions of the Arabian Sea, *Tellus, Ser. B*, *49*, 417–428, 1997.

Satheesh, S. K., K. K. Moorthy, and B. V. Murthy, Spatial gradients in aerosol characteristics over the Arabian Sea and Indian Ocean, *J. Geophys. Res.*, *103*, 26,183–26,192, 1998.

Savoie, D. L., J. M. Prospero, and R. T. Nees, Nitrate, non-sea-salt sulfate, and mineral aerosol over the northwestern Indian Ocean, *J. Geophys. Res.*, *92*, 933–942, 1987.

Siefert, R. L., A. M. Johansen, and M. R. Hoffmann, Chemical characterization of ambient aerosol collected during the southwest and intermonsoon seasons over the Arabian Sea: Labile-Fe(II) and other trace metals, *J. Geophys. Res.*, *104*, 3511–3526, 1999.

Taylor, S. R., and S. M. McLennan, *The Continental Crust: Its Composition and Evolution*, Blackwell Sci., Malden, Mass., 1985.

Tindale, N. W., and P. P. Pease, Aerosols over the Arabian Sea: Atmospheric transport pathways and concentrations of dust and sea salt, *Deep Sea Res., Part II*, *46*, 1577–1595, 1999.

Venkataraman, C., P. Sinha, and S. Bammi, Sulphate aerosol size distributions at Mumbai, India, during the INDOEX-FFP [1998], *Atmos. Environ.*, *35*(15), 2647–2655, 2001.

Venkataraman, C., C. Reddy, S. Josson, and M. Reddy, Aerosol size and chemical characteristics at Mumbai, India, during the INDOEX-IFP [1999], *Atmos. Environ.*, *36*(12), 1979–1997, 2002.

Wells, M. L., N. M. Price, and K. W. Bruland, Iron chemistry in seawater and its relationship to phytoplankton: A workshop report, *Mar. Chem.*, *48*, 157–182, 1995.

Zhu, X., J. M. Prospero, D. L. Svoie, F. J. Millero, R. G. Zika, and E. S. Saltzman, Photoreduction of iron(III) in marine mineral aerosol solutions, *J. Geophys. Res.*, *98*, 9039–9046, 1993.

Zhu, X. R., J. M. Prospero, and F. J. Millero, Diel variability of soluble Fe(II) and soluble total Fe in North African dust in the trade winds at Barbados, *J. Geophys. Res.*, *102*, 21,297–21,305, 1997.

Zhuang, G., Z. Yi, R. A. Duce, and P. R. Brown, Link between iron and sulphur cycles suggested by detection of Fe(II) in remote marine aerosols, *Nature*, *355*, 537–539, 1992.

A. M. Johansen, Department of Chemistry, Central Washington University, 400 East 8th Avenue, Ellensburg, WA 98926, USA. (johansea@cwu.edu)

M. R. Hoffmann, Environmental Science and Engineering, California Institute of Technology, Keck 138-78, Pasadena, CA 91125, USA. (mrh@caltech.edu)